Semiconductor Detectors Allow Low-Dose–Low-Dose 1-Day SPECT Myocardial Perfusion Imaging

Rene Nkoulou[*1], Aju P. Pazhenkottil[*1], Silke M. Kuest[1], Jelena R. Ghadri[1], Mathias Wolfrum[1], Lars Husmann[1], Michael Fiechter[1], Ronny R. Buechel[1], Bernhard A. Herzog[1], Pascal Koepfli[1], Cyrill Burger[1], Oliver Gaemperli[†1], and Philipp A. Kaufmann[†1,2]

[1]*Deparment of Radiology, Cardiac Imaging, University Hospital Zurich, Zurich, Switzerland; and* [2]*Zurich Centre for Integrative Human Physiology (ZIHP), University of Zurich, Zurich, Switzerland*

Cadmium zinc telluride (CZT) detectors with linear counting rate response enable count subtraction in sequential scanning. We evaluated whether count subtraction eliminated the need for higher activity doses in the second part of the 1-d stress–rest myocardial perfusion imaging (MPI) protocol. **Methods:** For 50 patients (mean age ± SD, 66 ± 12 y) with visually abnormal (n = 42) or equivocal (n = 8) adenosine-stress MPI (320 MBq of ^{99m}Tc-tetrofosmin) on a CZT camera, rest MPI was performed with a low dose (320 MBq) and repeated after injection of an additional 640 MBq of ^{99m}Tc-tetrofosmin to achieve a standard 3-fold increased dose at rest (960 MBq), compared with stress (320 MBq). Low-dose rest myocardial perfusion images were reconstructed after subtracting the background activity of the preceding stress scan. Segmental percentage tracer uptake of the 2 rest myocardial perfusion images (320 vs. 960 MBq) was compared using intraclass correlation and Bland–Altman limits of agreement. Patient- and coronary territory–based clinical agreement was assessed. **Results:** The standard protocol revealed ischemia in 34 (68%) and a fixed defect in 8 (16%) patients, of whom 33 (97%) and 8 (100%) were correctly identified by low-dose MPI (clinical agreement, 98%). Segmental uptake correlated well between low- and standard-dose rest scans (r = 0.94, $P <$ 0.001; Bland–Altman limits of agreement, −11 to +11%). Defect extent was 14.4% (low-dose) versus 13.1% (standard-dose) at rest (P = not statistically significant) and 26.6% at stress ($P <$ 0.001 vs. rest scans). **Conclusion:** These promising results suggest that accurate assessment of ischemic myocardial disease is feasible with a low-dose–low-dose 1-d SPECT MPI protocol using a CZT device.

Key Words: low-dose myocardial perfusion SPECT; cadmium-zinc-telluride detectors (CZT); background activity subtraction

J Nucl Med 2011; 52:1204–1209
DOI: 10.2967/jnumed.110.085415

Although invasive coronary angiography is regarded as the standard of reference for anatomic coronary artery disease (CAD) evaluation, functional assessment of hemodynamic lesion severity is essential for targeted revascularization strategies (*1,2*). In this context, myocardial perfusion imaging (MPI) with SPECT is the most widely used and best established tool for functional CAD assessment, providing accurate diagnostic and prognostic information. Over the last 3 decades, there has been a 6-fold increase in the radiation dose from medical imaging delivered to the patient (*3*). It is therefore conceivable that the radiation exposure experienced by patients undergoing any medical imaging procedure has recently gained growing attention and publicity (*4–6*), increasing the search for options to reduce radiation dose in SPECT MPI while maintaining diagnostic image quality. Various approaches have been suggested, such as improvements in iterative reconstruction techniques (*6–8*), dose-saving algorithms (*9*), and stress-only protocols (*10,11*). The latter, however, are not helpful in many instances in which information on reversibility of a perfusion defect is mandatory for evidence-based therapeutic decision making. Although the 1-d protocol for MPI is the preferred protocol in many centers because of its convenience, so far one of its major disadvantages has been the need for a 2- to 3-fold increase in tracer activity for the second scan to avoid shine-through effects from the first scan.

Recently, a new γ-camera generation with cadmium-zinc-telluride (CZT) detectors was introduced. The miniaturization of the semiconductors (*12*) has enabled a compact detector alignment, allowing the engineering of a circular and therefore stationary detector array, thus shortening the scan time substantially (*13,14*). Moreover, CZT detectors offer multiplied count sensitivity and provide a linear counting rate response. By contrast, conventional γ-cameras equipped with sodium iodide scintillators and photomultiplier tubes suffer from significant dead-time losses and occasionally even detector paralysis, which accounts for their nonlinear response particularly at high counting rates (*15*). A linear counting rate response, however, is an important

Received Nov. 17, 2010; revision accepted May 18, 2011.
For correspondence or reprints contact: Philipp A. Kaufmann, Department of Radiology, Cardiac Imaging, University Hospital Zurich, Rämistrasse 100, CH- 8091 Zurich, Switzerland.
E-mail: pak@usz.ch
*Contributed equally to this work as first coauthors.
†Contributed equally to this work as senior coauthors.

prerequisite for accurate background activity subtraction and may therefore pave the way for sequential low-dose scanning in MPI. Therefore, the aim of the present study was to evaluate whether the use of CZT detector technology coupled with background activity subtraction eliminates the need for high-dose injections in the second part of a 1-d stress–rest MPI protocol.

MATERIALS AND METHODS

Patient Population

Fifty patients scheduled for a 1-d stress–rest SPECT MPI scan for suspected or known CAD were prospectively enrolled. Inclusion criteria were visually abnormal or equivocal stress MPI after iterative reconstruction with and without CT attenuation correction. Patients with unequivocally normal stress MPI were excluded from the present study. The study protocol was approved by the institutional ethics committee, and written informed consent was obtained from each study participant.

Study Protocol and MPI Acquisition

Patients were advised to refrain from theophylline or caffeine-containing beverages for at least 12 h before the study. Pharmacologic stress was performed with adenosine infused at a rate of 140 μg/kg/min during 6 min, and a standard dose of 320 MBq of ^{99m}Tc-tetrofosmin was injected 3 min into the pharmacologic stress. Approximately 60 min later, stress myocardial perfusion images were acquired on a hybrid SPECT/CT scanner (DNM/CT 570c; GE Healthcare) integrating a CZT γ-camera and a 64-slice CT device. Thereafter, electrocardiogram-gated rest MPI was performed as proposed by Giorgetti et al. (*16*) after administration of 320 MBq of ^{99m}Tc-tetrofosmin and repeated after injection of an additional 640 MBq of ^{99m}Tc-tetrofosmin in the same session to achieve a 3-fold increased total ^{99m}Tc activity dose (i.e., 960 MBq) at rest, compared with stress MPI (320 MBq). All scans were acquired over 5 min in the SPECT part of the hybrid device, which is a γ-camera with a pinhole collimator and 19 stationary detector modules positioned around the patient's chest as previously described (*13,15*). A schematic representation of the acquisition protocol is illustrated in Figure 1.

MPI Reconstruction

All SPECT images were reconstructed using a commercially available dedicated software package (Myovation for Alcyone; GE Healthcare) with a new iterative algorithm based on integrated collimator geometry modeling, using maximum-penalized likelihood iterative reconstruction to obtain perfusion images in standard axes as previously reported (*13*). In brief, 40 and 50 iterations of the algorithm were used for reconstruction of the stress and rest datasets, respectively. A Butterworth postprocessing filter was applied (cutoff frequency, 0.37 cycle/cm; order, 7) to the reconstructed slices. For attenuation correction, a prospectively triggered CT scan was acquired at inspiratory breath-hold (2.5-mm section thickness, 0.35-s gantry rotation time, 120 kV, and 200–250 mA, depending on the patient's size) and reconstructed as previously reported (*17,18*).

Subtraction of Background Activity

Background activity was subtracted from the low-dose rest examination using the commercially available PMOD software package (version 3.2, PCARD; PMOD Technologies Ltd.). To this end, the low-dose rest and stress MPI datasets were processed with the PMOD fusion tool as previously validated (*19*). After a subtraction algorithm (rest low-dose minus stress) was applied, negative regional counts were set to zero. The resulting datasets were transferred to the Myovation for Alcyone software for further processing and image analysis.

SPECT Data Analysis

A perfusion polar map was displayed using a 17-segment model representation of the left ventricle (*20*), and segmental uptake values (percentage of maximum uptake) as well as extent of perfusion abnormalities at stress and rest, including its reversibility, were calculated. A semiquantitative score (0–4) for severity of perfusion abnormalities was computed on the basis of segmental uptake values: uptake greater than 70% (score, 0), 50%–70% (score, 1), 49%–30% (score, 2), 29%–10% (score, 3), and less than 10% (score, 4). The summed rest scores (SRSs) were assessed from low- and standard-dose scans and were subtracted from the summed stress scores (SSSs). to obtain summed difference scores (SDSs). An SSS of 4 or more was considered abnormal, and an SDS of 2 or more was considered to represent clinically relevant ischemia (*21–23*). In addition, segments 1, 2, 7, 8, 13, 14, and 17 were assigned to the left anterior descending territory; segments 3, 4, 9, 10, and 15 to the right coronary artery territory; and segments 5, 6, 11, 12, and 16 to the left circumflex territory to allow vessel-based comparison. Left ventricular (LV) volumes and ejection fraction were obtained using gated datasets reconstructed at 8 frames with the Quantitative Gated SPECT/Quantitative Perfusion SPECT software package (Cedars QGS/QPS; Cedars-Sinai Medical Center), which also provided the defect extent in percentage of LV myocardium. No subtraction was performed for the analysis of the gated dataset.

Torso Phantom Study

As preclinical validation, images were acquired using an anthropomorphic torso phantom (Radiologic Support Devices Inc.) with heart, lung, and liver inserts. The heart insert displays a volume of 238 mL and 284 mL, respectively, for myocardial wall and heart chambers. Two fillable defects were placed in the anteroseptal (30 mL) and inferolateral (13.5 mL) walls to simulate

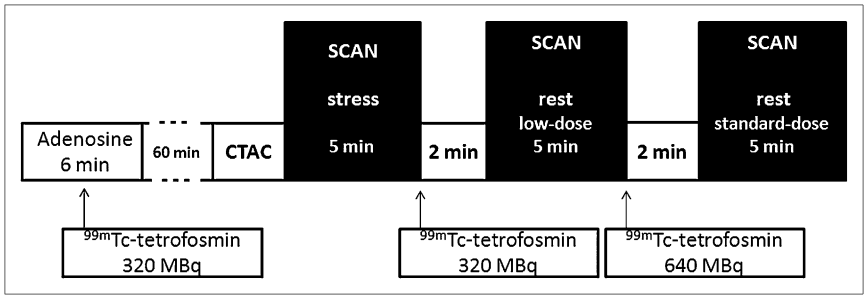

FIGURE 1. Schematic representation of acquisition protocol. CTAC = CT-based attenuation correction.

real perfusion abnormalities. The heart's radiotracer uptake at stress was estimated to account for 2% of the injected dose and 1% at rest. The heart-to-liver-to-background ratio was calculated according to Higley et al. and was 24:3:1 for the stress, 8:4.8:1 for the low-dose rest, and 6.7:7.6:1 for the standard-dose rest acquisitions (*24*). Stress defect was simulated using fillable defects without radiotracer activity. Rest uptake in ischemic areas was assumed to be normal, and the defect volume was filled with diluted ^{99m}Tc activity solution according to the rest activity provided (low-dose or standard). Serial acquisitions were performed to simulate a fixed inferolateral defect and a reversible anteroseptal defect under low-dose rest and standard-dose rest. An additional rest acquisition (rest only) with inferolateral defect but otherwise homogeneous activity was performed without preceding stress activity, to allow for the determination of the distribution of activity in the rest phantom without any shine-through effect from the preceding stress activity.

Statistical Analysis

All statistical evaluations were done using SPSS software (version 16.0.1 [SPSS Inc.] for Windows [Microsoft]). Categoric values were presented as proportions and percentages and continuous variables as mean ± SD or median with interquartile range, where appropriate. Segmental tracer uptake values were compared using intraclass correlation with 95% confidence interval (CI) and Bland–Altman limits of agreement (*25*). Paired data were compared with 2-tailed paired *t* test or Wilcoxon test as appropriate. Agreement rates on the clinical diagnosis between low-dose and standard-dose examinations were provided. A *P* value of less than 0.05 was considered statistically significant.

RESULTS

All 50 patients completed the stress and both rest imaging studies. The baseline characteristics of the study population are given in Table 1.

TABLE 1
Baseline Characteristics of Study Population (n = 50)

Characteristic	Value
Age (y)	
Mean	66
Range	39–86
Sex	
Male	35 (70)
Female	15 (30)
Body mass index	
Mean	26.2
Range	19–32
Risk factor	
Median	2
Range	1–4
Known CAD	31 (62)
Angina	
Typical	16 (32)
Atypical	18 (36)
Asymptomatic	16 (32)

Data in parentheses are percentages.

Patient-Based Comparison

The SRSs for the low-dose rest and standard rest examination were 3.8 ± 4.6 and 3.3 ± 4.5, respectively (P = not statistically significant [NS]), whereas SSS was 7.5 ± 4.9 ($P < 0.001$ vs. both SRSs). The standard protocol revealed ischemia in 34 (63%) and a fixed defect in 8 (16%) patients, of whom 33 (97%) and 8 (100%) were correctly identified by low-dose MPI. All 16 patients without ischemia on standard-dose rest examination also had no ischemia when using the low-dose rest examination, resulting in an overall clinical agreement rate of 98%. The only discordant result was found in a patient with an SSS of 12 in whom SDS was 1 in the low-dose examination and 2 in the standard-dose examination.

The difference in SRS between low-dose and standard-dose rest myocardial perfusion images ranged from −1 to +1 in 72% of the patients (Fig. 2). In the stress myocardial perfusion image, the mean extent of perfusion abnormality was 26.6% overall and 33.4% in ischemic patients. In the resting myocardial perfusion image with low-dose and standard-dose examination, the mean extent of rest perfusion abnormalities was 14.4% versus 13.1% overall, amounting to 16.6% versus 15.4% in ischemic patients, respectively (P = NS). The examinations resulted in an extent of reversible perfusion abnormalities (i.e., extent of ischemia) of 12.2% versus 13.5% overall and 16.8% versus 18.0%, respectively (P = NS) (Fig. 3). Without subtraction, low-dose results were significantly different from standard rest results, with an extent of rest perfusion abnormalities of 18% overall ($P = 0.004$ vs. standard rest) and 20.6% in ischemic patients ($P = 0.005$ vs. standard rest), resulting in a significant underestimation of the extent of ischemia both overall (8.6%) and in ischemic patients (12.8%) (both $P < 0.005$ vs. standard rest). Some illustrative cases of myocardial perfusion images obtained with low and standard doses are displayed in Figure 4.

Coronary Territory–Based Comparison

On coronary territory analysis, 105 coronary territories showed no reversible defects, including 97 normal and 8 fixed defects, whereas ischemia was found in 45 territories by the standard protocol. Visual evaluation showed no image degradation in previously normal territories by stress MPI. Agreement within 1 point (−1 to +1), between the low- and standard-dose protocols of the regional rest score, was 94% overall (Fig. 5).

Segmental Uptake Values

The intraclass correlation for segmental tracer uptake values between low-dose and standard-dose rest was 0.94 ($P < 0.001$; 95% CI, 0.93–0.95) overall and 0.94 ($P < 0.001$; 95% CI, 0.92–0.95), 0.91 ($P < 0.001$; 95% CI, 0.89–0.93), and 0.95 ($P < 0.001$; 95% CI, 0.94–0.96) in the segments of the left anterior descending, left circumflex, and right coronary artery territories, respectively. In segments without stress perfusion defect, the correlation in segmental tracer uptake with low-dose and standard-dose rest scan was 0.85 ($P < 0.001$; 95% CI, 0.82–0.87). The mean

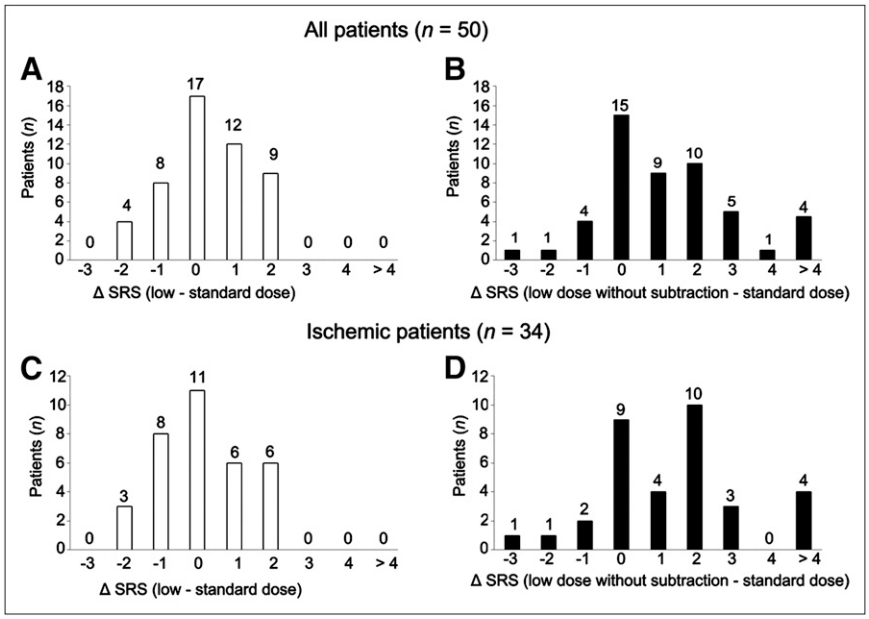

FIGURE 2. Difference (ΔSRS) between SRS of low-dose rest and standard-dose rest MPIs in all patients (A and B) and ischemic patients (C and D). In B and D, no subtraction of previous stress examination was performed, illustrating impact of shining through from previous stress examination on rest scan, limiting reversal of perfusion defect.

difference in tracer uptake between low- and standard-dose rest was −0.7% ± 5.1% for all segments, 1.5 ± 5.7 in segments with a score of 0, and −1.3 ± 6.0 in segments with score of 1 or more. Bland–Altman limits of agreement were −9 to +11, −12 to +9, and −10 to +13, respectively (Supplemental Fig. 1; supplemental materials are available online only at http://jnm.snmjournals.org).

LV Volumes and Ejection Fraction

For the low-dose rest and standard rest examinations, ejection fraction was 56% ± 18% versus 55% ± 17%, end-diastolic volume was 95 ± 50 versus 92 ± 46 mL, and end-systolic volume was 48 ± 45 versus 47 ± 43 mL, respectively (P = NS for all comparisons). Intraclass correlation between low-dose and standard rest examination for ejection fraction, end-diastolic volume, and end-systolic volume were 0.98 ($P < 0.001$; 95% CI, 0.96–0.99), 0.97 ($P < 0.001$; 95% CI, 0.95–0.99), and 0.99 ($P < 0.001$; 95% CI, 0.98–0.98), respectively (Supplemental Fig. 2).

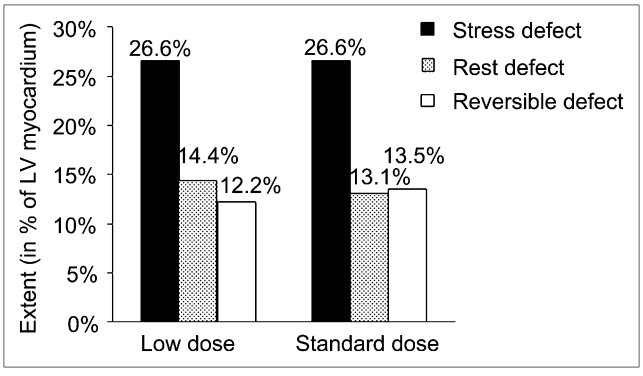

FIGURE 3. Extent of rest perfusion defect and defect reversibility (ischemia) with low-dose was highly comparable with standard-dose rest examination (P = NS). Values are given as percentage of total LV myocardium.

Torso Phantom Study

The rest-only phantom acquisition, simulating inferolateral defect without shine-through effect, also presented with a minimal apical–anteroseptal filling defect because of an inhomogeneity of the cardiac insert; this inhomogeneity was taken into consideration when interpreting subsequent acquisitions. Table 2 summarizes the scores of perfusion abnormalities obtained during the phantom study. Torso phantom reconstructions obtained from simulated stress, low-dose rest, and standard-dose rest scans are displayed in Supplemental Figure 3.

DISCUSSION

The results of the present study demonstrate that the novel DNM/CT 570c camera (equipped with CZT detector tech-

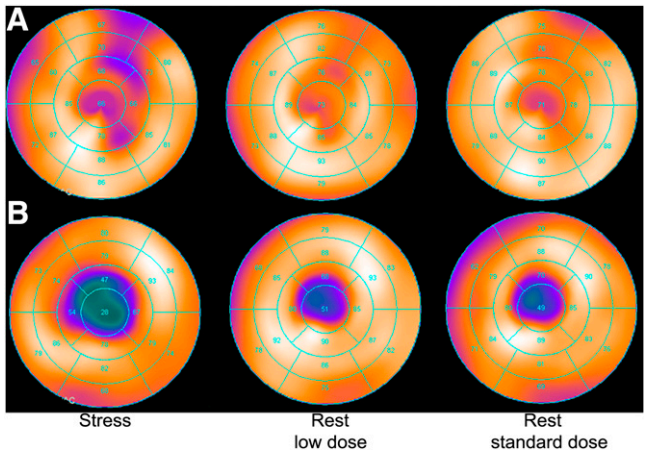

FIGURE 4. Illustrative cases of myocardial perfusion images obtained with low and standard doses. (A) Patient with stress perfusion defect that is entirely reversible at low- and standard-dose rest perfusion. (B) Patient with large apical defect partly reversible at rest. Fixed defect at rest is almost identical in low- vs. standard-dose rest perfusion.

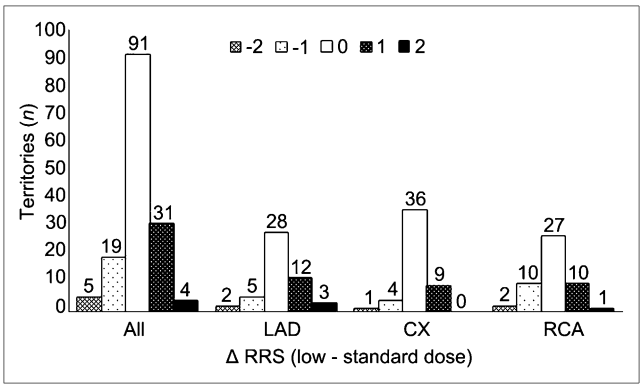

FIGURE 5. Difference between regional rest scores (ΔRRS) of low-dose rest and standard-dose rest myocardial perfusion images in coronary territories. CX = left circumflex; LAD = left anterior descending; RCA = right coronary artery; RRS = regional rest score.

nology) allows accurate CAD assessment using a low-dose–low-dose 1-d nuclear MPI protocol. Low-dose rest MPI provided clinical information equivalent to that from standard-dose rest MPI with regard to defect extent and severity. In conjunction with stress MPI, our protocol resulted in an excellent clinical agreement (98%) for myocardial ischemia evaluation, comparing well to the test–retest agreement reported in large trials (*6,26*). This agreement was maintained in a subgroup of 8 patients with borderline stress scans, in which minor differences in regional perfusion between low-dose and standard protocol may considerably affect the interpretation of the scan in favor of a normal or abnormal result. Furthermore, regional evaluation of ischemia revealed that the difference in regional scores between the standard- and the low-dose rest protocol did not exceed 2 (an appropriate cutoff value for clinical relevance) in any of the patients (*19*). The results of the clinical study were corroborated by a phantom study showing comparable fixed and reversible perfusion defects as well as equivalent shine-through from a previous scan when low-dose–low-dose or standard low-dose–high-dose simulations were performed. With regard to functional data, the novel low-dose–low-dose protocol, as compared with the standard protocol, also allows accurate assessment of LV volumes and ejection fraction. This is of great clinical importance not only because the LV function is a strong predictor of outcome but also because of the added value of wall motion analysis for discrimination of artifact from scar (*27*).

The quasilinear counting rate response, a distinct feature of CZT detectors facilitated by their short dead-time, allows reliable subtraction of background activity from the low-dose rest images (*15*). This characteristic avoids the necessity of injecting a high dose at rest to overcome background activity present from the initial stress injection. Because of the overaging of the general population—a consequence of ever-improving cardiovascular prevention and treatment strategies—an increasing number of CAD patients will undergo repeated noninvasive testing for treatment monitoring, particularly in the case of recurrent ischemia. It is in this context that the results of the present study may have a great clinical impact. First, the low-dose protocol reduces the total radiation dose to each patient per scan, a benefit that is multiplied in the case of repeated scanning during many years of follow-up. This scenario appears realistic for a disease such as CAD, because despite successful interventional treatment options, the underlying atherosclerotic process may be slowed but not eliminated. Indeed, this novel protocol reduces patient radiation exposure by half. Second, in view of the current worldwide shortage of ^{99}Mo, a low-dose–low-dose MPI SPECT protocol would contribute to important savings in ^{99m}Tc and a more economical use of the tracer.

It may be perceived as a potential limitation of our study that the extent of reversibility in those patients with inducible ischemia was large. Nonetheless, we included 8 patients with equivocal perfusion defects to ascertain the effect of the low-dose–low-dose subtraction protocol on rather ambivalent interpretations. Although the clinical relevance of smaller, potentially equivocal perfusion defects is minor, our results indicate similar clinical performance of the low-dose–low-dose protocol compared with the standard protocol in patients with borderline findings. If confirmed by larger trials, including in normal patients and also using rest–stress protocol MPIs, the low-dose–low-dose protocol could help to reduce radiation exposure and improve patient throughput in diagnostic nuclear cardiac imaging centers.

Furthermore, the interval between the low-dose injection and the start of image acquisition was low in the present study. However, it has been recently shown that with an interval of 5 min between injection and acquisition, adequate images can be obtained (*16*). Nevertheless, prolonging the delay may have further improved the image quality and, thus, would have further strengthened the results of the present study.

TABLE 2
Scores of Perfusion Abnormalities During Phantom Study

LV territory	Stress only	Rest only	Rest low-dose after stress	Rest standard-dose after stress
Left anterior descending	12	0	2	2
Left circumflex	4	5	4	3
Right coronary artery	3	4	3	3
All	19	9	9	8

Scores at stress and rest are SSS and SRS.

An additional potential limitation could arise from the stress–rest sequence of the 1-d protocol because in theory shine-through of the initial stress scan into the subsequent resting scan cannot be entirely excluded. However, as a systematic analysis of the stress–rest versus rest–stress sequence had not revealed any significant difference in accuracy in detecting ischemia (*28*), the guidelines of the European Association of Nuclear Medicine (*29*) supports the stress–rest sequence, which was used in the present study.

Finally, we did not compare the low-dose–low-dose protocol with invasive coronary angiography as standard of reference to determine the diagnostic performance for detecting CAD. Nonetheless, the excellent agreement with the standard protocol indicates that diagnostic performance will be in the range of previously published reports with standard SPECT MPI (*30*).

CONCLUSION

Accurate assessment of ischemic myocardial disease is feasible with a low-dose–low-dose 1-d SPECT MPI protocol using background activity subtraction on a CZT scanner.

DISCLOSURE STATEMENT

The costs of publication of this article were defrayed in part by the payment of page charges. Therefore, and solely to indicate this fact, this article is hereby marked "advertisement" in accordance with 18 USC section 1734.

ACKNOWLEDGMENTS

We thank Ennio Mueller, Edlira Loga, Mirjam De Bloeme, Sabrina Epp, and Patrick von Schulthess for their excellent technical support. We are also grateful to Osman Ratib and Habib Zaïdi (University Hospital of Geneva, Switzerland) for providing the torso phantom. The study was supported in part by a grant from the Swiss National Science Foundation (SNSF). No other potential conflict of interest relevant to this article was reported.

REFERENCES

1. Tonino PA, De Bruyne B, Pijls NH, et al. Fractional flow reserve versus angiography for guiding percutaneous coronary intervention. *N Engl J Med.* 2009; 360:213–224.
2. Kern MJ, Lerman A, Bech JW, et al. Physiological assessment of coronary artery disease in the cardiac catheterization laboratory: a scientific statement from the American Heart Association Committee on Diagnostic and Interventional Cardiac Catheterization, Council on Clinical Cardiology. *Circulation.* 2006;114: 1321–1341.
3. Brenner DJ, Hall EJ. Computed tomography: an increasing source of radiation exposure. *N Engl J Med.* 2007;357:2277–2284.
4. Lauer MS. Elements of danger: the case of medical imaging. *N Engl J Med.* 2009;361:841–843.
5. Kaufmann PA, Knuuti J. Ionizing radiation risks of cardiac imaging: estimates of the immeasurable. *Eur Heart J.* 2010;31:9–11.
6. Ali I, Ruddy TD, Almgrahi A, Anstett FG, Wells RG. Half-time SPECT myocardial perfusion imaging with attenuation correction. *J Nucl Med.* 2009;50:554–562.
7. Valenta I, Treyer V, Husmann L, et al. New reconstruction algorithm allows shortened acquisition time for myocardial perfusion SPECT. *Eur J Nucl Med Mol Imaging.* 2010;37:750–757.
8. Borges-Neto S, Pagnanelli RA, Shaw LK, et al. Clinical results of a novel wide beam reconstruction method for shortening scan time of Tc-99m cardiac SPECT perfusion studies. *J Nucl Cardiol.* 2007;14:555–565.
9. Pazhenkottil AP, Herzog BA, Husmann L, et al. Non-invasive assessment of coronary artery disease with CT coronary angiography and SPECT: a novel dose-saving fast-track algorithm. *Eur J Nucl Med Mol Imaging.* 2010;37:522–527.
10. Husmann L, Herzog BA, Gaemperli O, et al. Diagnostic accuracy of computed tomography coronary angiography and evaluation of stress-only single-photon emission computed tomography/computed tomography hybrid imaging: comparison of prospective electrocardiogram-triggering vs. retrospective gating. *Eur Heart J.* 2009;30:600–607.
11. Duvall WL, Wijetunga MN, Klein TM, et al. The prognosis of a normal stress-only Tc-99m myocardial perfusion imaging study. *J Nucl Cardiol.* 2010;17:370–377.
12. Madsen MT. Recent advances in SPECT imaging. *J Nucl Med.* 2007;48:661–673.
13. Herzog BA, Buechel RR, Katz R, et al. Nuclear myocardial perfusion imaging with a cadmium-zinc-telluride detector technique: optimized protocol for scan time reduction. *J Nucl Med.* 2010;51:46–51.
14. Buechel RR, Herzog BA, Husmann L, et al. Ultrafast nuclear myocardial perfusion imaging on a new gamma camera with semiconductor detector technique: first clinical validation. *Eur J Nucl Med Mol Imaging.* 2010;37:773–778.
15. Bocher M, Blevis IM, Tsukerman L, Shrem Y, Kovalski G, Volokh L. A fast cardiac gamma camera with dynamic SPECT capabilities: design, system validation and future potential. *Eur J Nucl Med Mol Imaging.* 2010;37:1887–1902.
16. Giorgetti A, Rossi M, Stanislao M, et al. Feasibility and diagnostic accuracy of a gated SPECT early-imaging protocol: a multicenter study of the Myoview Imaging Optimization Group. *J Nucl Med.* 2007;48:1670–1675.
17. Schepis T, Gaemperli O, Koepfli P, et al. Use of coronary calcium score scans from stand-alone multislice computed tomography for attenuation correction of myocardial perfusion SPECT. *Eur J Nucl Med Mol Imaging.* 2007;34:11–19.
18. Herzog BA, Buechel RR, Husmann L, et al. Validation of CT attenuation correction for high-speed myocardial perfusion imaging using a novel cadmium-zinc-telluride detector technique. *J Nucl Med.* 2010;51:1539–1544.
19. Adachi I, Gaemperli O, Valenta I, et al. Assessment of myocardial perfusion by dynamic O-15-labeled water PET imaging: validation of a new fast factor analysis. *J Nucl Cardiol.* 2007;14:698–705.
20. Cerqueira MD, Weissman NJ, Dilsizian V, et al. Standardized myocardial segmentation and nomenclature for tomographic imaging of the heart: a statement for healthcare professionals from the Cardiac Imaging Committee of the Council on Clinical Cardiology of the American Heart Association. *Int J Cardiovasc Imaging.* 2002;18:539–542.
21. Reyes E, Stirrup J, Roughton M, D'Souza S, Underwood SR, Anagnostopoulos C. Attenuation of adenosine-induced myocardial perfusion heterogeneity by atenolol and other cardioselective beta-adrenoceptor blockers: a crossover myocardial perfusion imaging study. *J Nucl Med.* 2010;51:1036–1043.
22. Hachamovitch R, Berman DS, Shaw LJ, et al. Incremental prognostic value of myocardial perfusion single photon emission computed tomography for the prediction of cardiac death: differential stratification for risk of cardiac death and myocardial infarction. *Circulation.* 1998;97:535–543.
23. Sharir T, Germano G, Kang X, et al. Prediction of myocardial infarction versus cardiac death by gated myocardial perfusion SPECT: risk stratification by the amount of stress-induced ischemia and the poststress ejection fraction. *J Nucl Med.* 2001;42:831–837.
24. Higley B, Smith FW, Smith T, et al. Technetium-99m-1,2-bis[bis(2-ethoxyethyl) phosphino]ethane: human biodistribution, dosimetry and safety of a new myocardial perfusion imaging agent. *J Nucl Med.* 1993;34:30–38.
25. Bland JM, Altman DG. Statistical methods for assessing agreement between two methods of clinical measurement. *Lancet.* 1986;1:307–310.
26. Iskandrian AE, Bateman TM, Belardinelli L, et al. Adenosine versus regadenoson comparative evaluation in myocardial perfusion imaging: results of the ADVANCE phase 3 multicenter international trial. *J Nucl Cardiol.* 2007;14:645–658.
27. Fleischmann S, Koepfli P, Namdar M, Wyss CA, Jenni R, Kaufmann PA. Gated ^{99m}Tc-tetrofosmin SPECT for discriminating infarct from artifact in fixed myocardial perfusion defects. *J Nucl Med.* 2004;45:754–759.
28. Heo J, Kegel J, Iskandrian AS, Cave V, Iskandrian BB. Comparison of same-day protocols using technetium-99m-sestamibi myocardial imaging. *J Nucl Med.* 1992; 33:186–191.
29. Hesse B, Tagil K, Cuocolo A, et al. EANM/ESC procedural guidelines for myocardial perfusion imaging in nuclear cardiology. *Eur J Nucl Med Mol Imaging.* 2005;32:855–897.
30. Klocke FJ, Baird MG, Lorell BH, et al. ACC/AHA/ASNC guidelines for the clinical use of cardiac radionuclide imaging: executive summary: a report of the American College of Cardiology/American Heart Association Task Force on Practice Guidelines (ACC/AHA/ASNC Committee to Revise the 1995 Guidelines for the Clinical Use of Cardiac Radionuclide Imaging). *J Am Coll Cardiol.* 2003;42:1318–1333.